Quantitative analysis of resonant third-harmonic generation in strontium

H. Scheingraber, H. Puell, and C. R. Vidal
Max-Planck-Institut für Extraterrestrische Physik, Garching, Germany
(Received 14 November 1977)

Absolute intensity measurements of resonant third-harmonic generation in a Sr-Xe mixture have been performed using a flash-lamp-pumped dye laser. The third-harmonic power increased by about 3 orders of magnitude with respect to the pure Sr system by adjusting a pressure ratio of $p_{Xe}/p_{Sr} = 53$. Excellent agreement with theory is obtained provided the absorption cross section $\sigma_3 = 3.5 \times 10^{-18}$ cm^2 of Sr at the third-harmonic wavelength of 191.97 nm has been taken into account. The absorption cross section limits the conversion efficiency to 2×10^{-5} for an input intensity of 5×10^6 W/cm^2. Up to these intensities no saturation effects were observed.

I. INTRODUCTION

In 1974, Hodgson, Sorokin, and Wynne[1] first reported efficient two-photon resonant third-harmonic-generation (THG) and sum frequency mixing in a Sr-Xe mixture. Since then, resonantly enhanced four-wave processes in Na,[2] Cs,[3,4] Tl,[5] Mg,[6] and Ca,[7] have been reported. Most of these experiments were performed using high intensities in order to achieve high conversion efficiencies and/or to study saturation effects. Sum frequency mixing in Sr in the picosecond domain was investigated by Royt and Lee.[8]

For efficient harmonic generation the nonlinear system should be phase matched. Two different methods of phase matching are shown to be feasible. In the case of resonantly enhanced harmonic generation Bjorklund *et al.*[9] obtained phase matching by adjusting the frequencies of the fundamental waves in a single-component system. They also applied their method to strontium.[10] The other method performs phase matching by a proper adjustment of the partial pressures in a two-component system.[11] The latter technique is used in our experiments and for resonant THG a detailed quantitative agreement has been achieved for the first time which so far has only been obtained for nonresonant systems.[12]

We present experimental results for resonant THG in a Sr-Xe mixture using a flash-lamp pumped dye laser with peak powers up to 40 kW. A theoretical analysis is given including absorption effects which are demonstrated to play an important role in the Sr-Xe system. Modifications with respect to the analysis of the Rb-Xe system by Puell *et al.*[12] were made taking into account the two-photon resonance and the absorption of the generated vacuum-ultraviolet (vuv) radiation. In this manner excellent agreement between theory and experiment is obtained.

Section II contains a theoretical analysis and presents the results of numerical calculations in which the effects of density gradients at the boundary layers of the Sr vapor column in a heat-pipe oven are included. In addition, numerical values for the required linear and nonlinear susceptibilities are presented. In Sec. III the experimental setup is described and in Sec. IV the experimental results and a comparison with the theory are presented.

II. THEORY

For the theoretical analysis of THG in an absorbing medium we start from the linearized wave equation [see, for example, Eq. (19) of Ref. 12]. For a parallel beam and at powers sufficiently low to neglect self-action effects ($\vec{P}_q^s = 0$), the amplitude of the third-harmonic field is given by

$$\frac{d\hat{E}_3}{dz} = i\frac{9\omega^2\pi N}{2c^2 k_3}\chi_T^{(3)}(3\omega)\hat{E}_1^3 e^{i\Delta kz} - \hat{E}_3\left(\frac{\alpha_3}{2} + iz\frac{dk_3}{dz}\right), \tag{1}$$

where we also neglected depletion and absorption of the fundamental wave ($d\hat{E}_1/dz = 0$, small-signal approximation). $\chi_T^{(3)}(3\omega)$ is the nonlinear susceptibility responsible for THG, $\hat{E}_1$ and $\hat{E}_3$ are the amplitudes of the incoming and of the generated harmonic electric field, respectively, $\Delta k = 3k_1 - k_3$ is the mismatch of the corresponding wave vectors, α_3 is the absorption coefficient for the third-harmonic radiation, and N is the particle density of the nonlinear medium. For a homogeneous nonlinear medium [$N(z) = \text{const.}$], Eq. (1) can be integrated in closed form as shown for the first time by Bey *et al.*[13] who investigated THG in liquids. One obtains for the third-harmonic intensity

$$\Phi_3 = \left(\frac{24\pi^3\tilde{\nu}}{c}\left|\chi_T^{(3)}(3\omega)\right|\right)^2 \frac{\Phi_1^3}{n_3 n_1^3}\frac{1}{(\frac{1}{2}\sigma_3)^2 + (\Delta k/N)^2} \times \left[1 + e^{-NL\sigma_3} - 2e^{-NL\sigma_3/2}\cos(\Delta kL)\right] \tag{2}$$

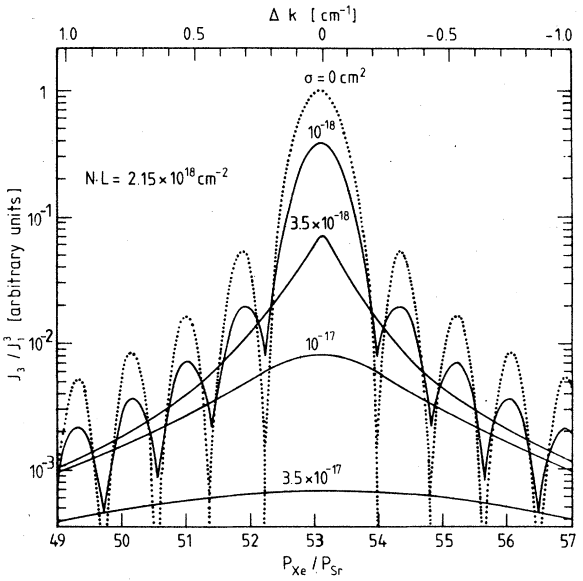

FIG. 1. Normalized third harmonic energy J_3/J_1^3 vs Xe-Sr pressure ratio for $NL = 2.15 \times 10^{18}$ cm^{-2} and different values of the absorption cross section σ_3. The corresponding mismatch Δk is shown on the top. (Rectangular density distribution.)

with $\Phi_q = (n_q c/8\pi)|E_q|^2$ and $\sigma_3 = \alpha_3/N$. L is the length of the nonlinear medium and $\tilde{\nu}$ is the wave number of the fundamental wave. For $\sigma_3 = 0$, Eq. (2) yields the well-known small-signal relation

$$\Phi_3 = \left(\frac{24\pi^3 NL\tilde{\nu}}{c}\,|\chi_T^{(3)}(3\omega)|\right)^2 \frac{\Phi_1^3}{n_3 n_1^3}\left(\frac{\sin(\frac{1}{2}\Delta kL)}{\frac{1}{2}\Delta kL}\right)^2 . \tag{3}$$

We will now investigate the dependence of the generated third-harmonic energy on the mismatch Δk and on the optical depth $\tau_3 = NL\sigma_3$ given by Eq. (2). Figure 1 shows the third-harmonic energy J_3 normalized with respect to the third power of the fundamental energy J_1 vs Δk for several values of σ_3. The value for NL (2.15×10^{18} cm^{-2}) was chosen according to our experimental conditions presented below. The dotted line shows the $[\sin(\frac{1}{2}\Delta kL)/(\frac{1}{2}\Delta kL)]^2$ behavior of the absorption-free case according to Eq. (3). In Fig. 1 the modulation of the phase-matching curve with the periodicity of $\Delta kL = 2n\pi$ decreases with an increasing absorption cross section σ_3. Eventually for $NL\sigma_3 \gg 1$, the phase-matching curve goes over to a pure dispersion-type curve where σ_3 acts as a damping constant. In this case the third-harmonic intensity Φ_3 becomes independent of the length L of the nonlinear medium. For $NL\sigma_3 \gg 1$

$$\Phi_3 = \left(\frac{24\pi^3\tilde{\nu}}{c}\,|\chi_T^{(3)}(3\omega)|\right)^2 \frac{\Phi_1^3}{n_3 n_1^3}\,\frac{1}{(\frac{1}{2}\sigma_3)^2 + (\Delta k/N)^2} . \tag{4}$$

Note that for a one-component system, where $\Delta k \sim N$, Eq. (4) is also independent of N. This behavior is illustrated in Fig. 2 where the normalized energy J_3 is plotted versus the length L for some values of σ_3. The mismatch ($\Delta k = 1.27$ cm^{-1}) and the particle density ($N = 7.15 \times 10^{16}$ cm^{-3}) are taken to be constant over the length of the nonlinear medium. Again the dotted line corresponds to the absorption-free case. Similar to Fig. 1 the damping of the modulation with increasing optical depth can be seen and it clearly reveals the effect of the absorption on the THG.

If the nonlinear medium is phase matched ($\Delta k = 0$) Eq. (2) yields

$$\Phi_3 = \left(\frac{48\pi^3\tilde{\nu}}{c\sigma_3}\,|\chi_T^{(3)}(3\omega)|\right)^2 \frac{\Phi_1^3}{n_3 n_1^3}(1 - e^{-NL\sigma_3/2})^2 . \tag{5}$$

For a strong absorption, $NL\sigma_3 \gg 1$, this expression becomes independent of the particle density and the length L of the nonlinear medium. For $\Delta k \ll \sigma_3 N$ and $NL\sigma_3 \gg 1$, we have

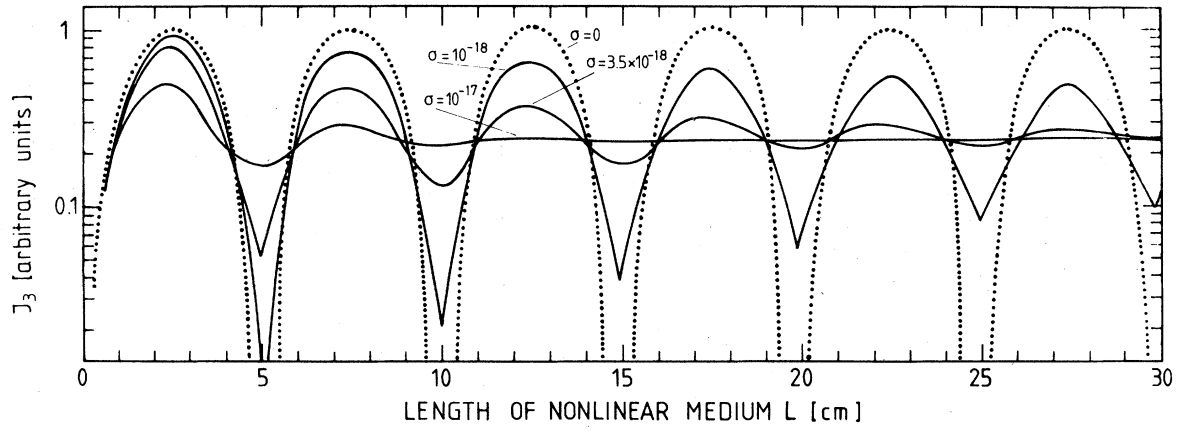

FIG. 2. Third harmonic energy J_3 vs length of the nonlinear medium for different values of the absorption cross section σ_3 and a constant mismatch $\Delta k = 1.27$ cm^{-1}. (Rectangular density distribution.)

$$\Phi_3 = \left(\frac{48\pi^3\tilde{\nu}}{c\sigma_3}\left|\chi_T^{(3)}(3\omega)\right|\right)^2 \frac{\Phi_1^3}{n_3 n_1^3}. \quad (6)$$

In this case the conversion efficiency is governed by the ratio of the nonlinear susceptibility $\chi_T^{(3)}(3\omega)$ and the absorption cross section σ_3 as already pointed out by Van Tran *et al.*[14] who investigated THG in InSb using a CO_2 laser.

The preceding relations have all been derived for a rectangular density profile with $N(z)$ = const over the length of the nonlinear medium. In practice however, the metal-vapor–noble-gas mixtures required for proper phase matching are produced, for example, in a concentric heat-pipe oven[15] where the small density gradients in the transition zones to the buffer gas have to be considered. These density gradients which may be approximated by $N(z) = \frac{1}{2}N(0)\{1 + \tanh[\alpha(\frac{1}{2}L - |z|)]\}$ modify the phase-matching curve as shown in Ref. 12.

To investigate this case, Eq. (1) had to be evaluated numerically. This was done for different optical depths. Figure 3 shows the results for $\tau_3 = 7.5$ and for different values α characterizing the steepness of the density gradients according to the corresponding diffusion coefficient. Similar to the absorption-free case, the curve becomes asymmetric with respect to Δk. The maximum is shifted to positive values of Δk and decreases with decreasing values of α.

To apply the preceding considerations to the special case of the two-photon-resonant THG, and to compare our measurements in Sr with theory, the effective two-photon-resonant third-order nonlinear susceptibility must be known. This nonlinear susceptibility $\chi_T^{(3)}(3\omega)$ is given to a good approximation at exact resonance by

$$\chi_T^{(3)}(3\omega) \simeq \hbar^{-3} \sum_{lmn} \frac{\mu_{0l}\mu_{lm}\mu_{mn}\mu_{n0}}{(\omega_{l0} - \omega)(\omega_{n0} - 3\omega)\Gamma_{\text{eff}}}, \quad (7)$$

where Γ_{eff} is the effective linewidth of the two-photon-resonant transition. In general, the value of Γ_{eff} depends on the Doppler width, the pressure broadening constant of the resonant transition, and on the linewidth of the laser.[16] For high-incident intensities Γ_{eff} becomes intensity dependent due to power broadening and Stark shifts[4] which turn out to be important in our experiments for incident intensities $\Phi_1 > 10^7$ W/cm^2. Other saturation effects such as two-photon absorption and/or three-photon ionization will modify the effective nonlinear susceptibility $\sum_i N_i \chi_{iT}^{(3)}$ according to the population densities N_i of the atomic states involved. Similarly saturation effects can also destroy the phase matching. In Eq. (7) the μ_{ik} are the dipole-moment matrix elements for transitions with the frequency ω_{ik} in the atoms of the nonlinear medium. In case of autoionizing states the matrix elements μ_{ik} can be evaluated according to Fano[17] as shown by Armstrong and Wynne.[18]

To calculate the nonlinear susceptibility $\chi_T^{(3)}$ the lowest lying S, P, and D energy levels of Sr (Ref. 19) (a total of 42) were taken into account. The corresponding matrix elements were evaluated in the Coulomb approximation. The agreement with measured values of the oscillator strength, even for the first resonance line [$f_{\text{cal}} = 1.93$, $f_{\text{meas}} = 1.92$ (Ref. 20)] is very good. In our calculations we neglected the Fano contribution since the wavelength of interest at 191.9 nm is sufficiently far off from the autoionizing transition around 197 nm. Further confidence in our approach is to some extent provided by the $\chi^{(1)}$ coefficients which are responsible for the excellent agreement of the measured and calculated phase-matching ratio $N_{\text{Xe}}/N_{\text{Sr}}$ (measured value: 53.0, calculated value: 53.1). Including the oscillator strength of the autoionizing transition around 197 nm according to Kozlov and Startsev[21] the calculated phase-matching ratio is changed by only 1%. The calculated linear and nonlinear susceptibilities of Sr for $\tilde{\nu} = 17\,363.74$ cm^{-1} and $3\tilde{\nu} = 52\,091.23$ cm^{-1} corresponding to the two-photon transition $5s^2$-$5s\,5d$ are given in Table I.

It is interesting to investigate the frequency dependence of Eq. (6) around a discrete transition at the frequency ω_{n0}. One obtains to a good approximation

$$\Phi_3 \sim (|\chi_T^{(3)}|/\sigma_3)^2 \sim [(\Omega_{n0} - 3\omega)^2 + \Gamma_{n0}^2]/\Gamma_{n0}^2, \quad (8)$$

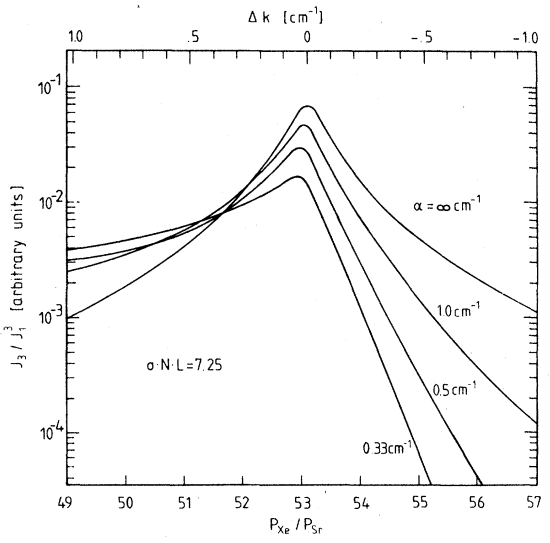

FIG. 3. Normalized third harmonic energy J_3/J_1^3 vs Xe-Sr pressure ratio for a constant optical depth $NL\sigma_3 = 7.25$ and different values of the density gradient α. $\alpha = \infty$ corresponds to a rectangular density distribution.

TABLE I. Linear susceptibilities $\chi^{(1)}(\omega)$ and $\chi^{(1)}(3\omega)$ for Sr and Xe (Ref. 25) and nonresonant and resonant part of the third-order susceptibility $\chi_T^{(3)}(3\omega)$ of Sr.

	$\chi^{(1)}(\omega)$ (10^{24} esu)	$\chi^{(1)}(3\omega)$ (10^{24} esu)	$[\chi_T^{(3)}(3\omega)]_{NR}$ (10^{32} esu)	$[\chi_T^{(3)}(3\omega)]_R$ (10^{32} esu)
Sr	81.87	−7.021	0.034	51.0
Xe	4.169	5.845		

where the complex frequency $\omega_{n0} = \Omega_{n0} + i\Gamma_{n0}$. Due to the absorption one therefore obtains an inverted dispersion profile which gives rise to a dip in the conversion efficiency. This statement has to be modified in case of autoionizing transition where the line shape of $\chi_T^{(3)}$ and σ_3 contained in the matrix elements μ_{ik}, may well be different since $\chi_T^{(3)} \sim \mu_{mn}\mu_{n0}$ and $\sigma_3 \sim \mu_{n0}^2$. It should be noted that Royt and Lee[8] observed a broad dip also for the autoionizing transition of Sr around 197 nm.

III. EXPERIMENTAL

The experimental arrangement is shown in Fig. 4. We used a flash-lamp pumped rhodamin 6G dye laser. The laser pulses had a duration of 500 nsec (FWHM) and an energy up to 20 mJ per pulse corresponding to a peak power of 40 kW. The dye cell inside the resonator was placed at Brewster's angle providing a linearly polarized beam. An interference filter and a Fabry Perot étalon inside the laser resonator were used to tune the wavelength to the $5s^2$-$5s\ 5d$ two-photon transition of strontium and to narrow the laser linewidth down to about 0.3 cm^{-1}.

The Sr vapor as the nonlinear medium was prepared in a concentric stainless-steel heat-pipe oven,[15] which allows the partial pressures of strontium and xenon to be varied independently without relying on any of the vapor pressure curves. With our heat-pipe system it was possible to adjust the Sr pressure typically between 6.5 and 20 torr and to change the length of the vapor column up to 45 cm. At lower pressures the heat pipe does no longer provide a stable operation any more because the Sr vapor starts to freeze out at the colder boundary layers between the vapor zone and the confining noble gas. (The Sr vapor pressure at the melting point of 785 °C is already 3.5 torr.). The upper limit of 20 torr corresponding to a temperature of 1000 °C is determined by the thermal stability of the stainless-steel structure. The Sr and Xe partial pressures were measured with an accuracy of 0.1% using commercial capacitive manometers.

Some problems may arise due to fog developing in the inner heat pipe, which contains some 100 torr of xenon as a phase-matching medium. Due to the relatively small heat conductivity of xenon, a weak temperature gradient from the wall to the center of the heat pipe can develop. Such a gradient tends to generate an oversaturated vapor in the central region. This oversaturated vapor condenses on the Sr ions generated by the absorption of the vuv radiation along the path of the laser beam and gives rise to Mie scattering. This effect limited the repetition rate of the laser to about 0.5 Hz. The fog is generally removed due to convection inside the inner heat pipe.

The laser beam was focused very weakly by a f = 100 cm lens to a spot area of 0.01 cm^2 (corresponding to a confocal parameter of 550 cm) into the heat pipe. The power of the incoming fundamental wave was measured by a calibrated fast photodiode, the power of the harmonic signal by a solar-blind photomultiplier after attenuating the signal by a factor of 10^{-4} to avoid saturation of the detector.

For determining the absorption cross section of Sr at 191.97 nm a small portion (7%) of the generated vuv radiation was reflected back into the heat pipe by means of a MgF_2 plate placed at the end of the heat pipe. The power of the reflected beam transmitted through the Sr vapor column was simultaneously monitored at the input side of the heat pipe using an additional solar-blind multiplier.

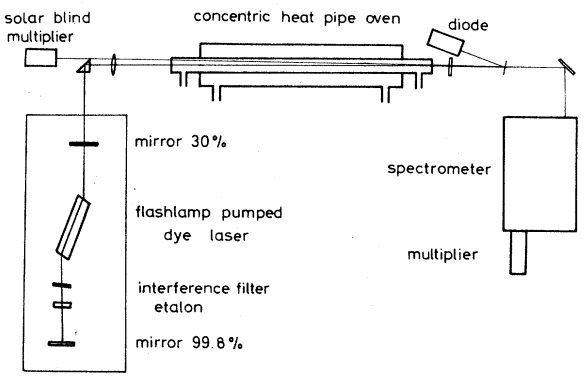

FIG. 4. Experimental arrangement consisting of a flash-lamp pumped dye laser, a concentric heat-pipe oven and the diagnostic system.

IV. RESULTS

The purpose of our experiments was to obtain a quantitative understanding of the two-photon resonant THG in a metal-vapor–noble-gas system. For the analysis of the system we performed all our measurements with a nearly parallel light beam. We investigated the phase-matching condition, the dependence of the third-harmonic power on the length and particle density of the active medium and on the power of the fundamental wave. Finally, we performed absolute power measurements to determine the conversion efficiency. The results of these measurements demonstrate the importance of the absorption of the generated vuv radiation in a Sr-Xe system for the phase-matching curve as well as for the absolute conversion efficiency.

In order to measure a phase-matching curve we started with a pure-strontium-vapor column at a pressure of 8.5 torr and a length of 30 cm. The measured third-harmonic power was normalized with respect to the third power of the fundamental power, and monitored as a function of the Xe pressure. The vuv signal increased slowly with increasing Xe pressure and reached a peak at a pressure ratio of $p_{Xe}/p_{Sr} = 53.0$. Higher Xe pressures caused a steep drop off in the THG. The power of the third-harmonic wave increased by about three orders of magnitude at optimum phase-matching compared to the harmonic power in pure strontium. Hodgson *et al.*[1] reported an increase by only a factor of 5. They also saw the steep drop off for high Xe pressures which so far has not been understood. In Fig. 5 the measured phase-matching curve around the optimum pressure ratio is shown. The curve is asymmetric and reveals the rather large density gradient as demonstrated in Fig. 3.

To compare our measurements with the calculations the values for the absorption cross section σ_3 of Sr and for the steepness of the density gradients (characterized by the quantity α) must be known. The absorption cross section was measured with the arrangement described in Sec. III. To eliminate contributions due to the transition zones, only differences in the optical depth were used to determine the cross section σ_3.[22] The length of the vapor column, determined by the temperature profile of the heat pipe, was measured with a pyrometer and varied between 25 and 40 cm at a pressure of 7 torr strontium and between 20 and 30 cm at a pressure of 12 torr. The incoming fundamental beam was attenuated to avoid THG of the beam which was reflected back through the heat pipe. The value of the absorption cross section of strontium at 191.97 nm measured

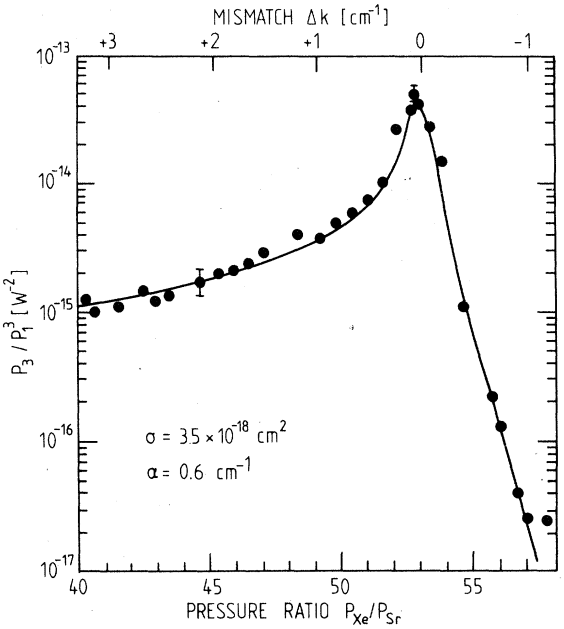

FIG. 5. Phase matching curve of the Sr-Xe system for a parallel beam. The theoretical curve is calculated for $NL\sigma_3 = 7.5$ and $\alpha = 0.6$ cm^{-1}.

in this way is $\sigma_3 = (3.5 \pm 1.0) \times 10^{-18}$ cm^2 in good agreement with the value given by Hudson *et al.*[23] and a factor of 3 lower than the value given by Kozlov and Startsev.[21]

The quantity α cannot be measured directly. But, as shown in Fig. 3, the asymmetry of the phase-matching curve is very sensitive to this value. The best fit of the measured curve was achieved for $\alpha = 0.6$ cm^{-1}. On the other hand it is possible to extrapolate the value of α, using the data of the Rb-Xe system[12] and the known dependence of the diffusion length on the reduced mass μ and on the temperature T, $\alpha \sim \sqrt{\mu/kT}$. This method yields a value $\alpha = 0.59$ cm^{-1} in very good agreement with the optimum fit. The solid line in Fig. 5 shows the calculated phase-matching curve using $\sigma_3 = 3.5 \times 10^{-18}$ cm^2, $\alpha = 0.6$ cm^{-1}, $L = 30$ cm, and $p_{Sr} = 8.5$ torr corresponding to a temperature of 865 °C. The agreement with the measured curve is excellent.

With these values of N, L, and σ_3 we have a typical optical thickness of $NL\sigma_3 \approx 7.5$. Hence, from Eq. (5) we expect the THG to be independent of N and L. In order to prove this point we changed the Sr pressure from 6.5 to 14 torr keeping the length of the vapor column constant at 30 cm and maintaining optimum phase matching. The generated harmonic power showed no significant increase. Furthermore, we kept the Sr pressure constant at 8.5 torr, adjusted the phase matching, and varied the length between 20 and 45 cm. Again no significant change of the third-harmonic power was ob-

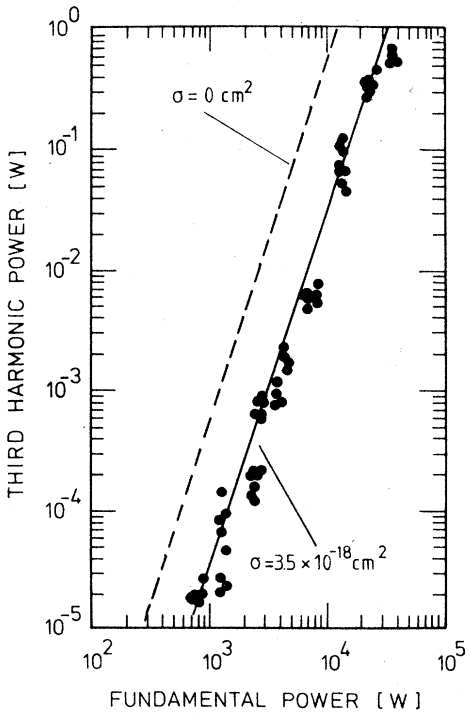

FIG. 6. Third harmonic power vs fundamental power. The dashed and the solid lines represent numerical calculations neglecting and including the absorption term.

served in accordance with our theoretical predictions.

To investigate the THG as a function of the input power we used neutral density filters to attenuate the fundamental power. The intensities of the harmonic and fundamental waves were monitored simultaneously on a dual-beam oscilloscope. The results are shown in Fig. 6, where the power of the third harmonic is plotted versus the power of the fundamental wave. Each point represents a single laser shot. Varying the input power from about 1 to 40 kW (corresponding to intensities from 1.2×10^5 to 5×10^6 W/cm^2) the third-harmonic power increases over the full intensity range proportional to the cube of the fundamental power. The maximum power conversion achieved was 2×10^{-5}.

For the comparison with our theoretical predictions the value of Γ_{eff} in Eq. (7) is needed. This value was determined to $\Gamma_{\text{eff}} = 0.4$ cm^{-1} by scanning the laser wavelength over the two-photon transition $5s^2$-$5s5d$ and monitoring the corresponding third-harmonic power. The corresponding results of numerical calculations using Eq. (1) are also shown in Fig. 6. Note that due to the multimode structure of our laser the single mode results of Eq. (1) have to be multiplied by a factor 3! (Ref. 26). The dashed line represents the result assuming a Gaussian radial intensity distribution and a density gradient of $\alpha = 0.6$ cm^{-1}, but neglecting any absorption processes. The solid line was obtained in the same manner, but including the third-harmonic absorption cross section of $\sigma_3 = 3.5\times10^{-18}$ cm^2. Since the third-harmonic power is independent of length and particle density of the nonlinear medium and since Γ_{eff} is determined experimentally all necessary parameters are specified and the solid line in Fig. 6 is obtained without fitting any free parameter.

V. SUMMARY

A detailed quantitative analysis of the third-harmonic generation in a Sr-Xe mixture has been carried out, using the two-photon transition $5s^2$-$5s\,5d$. The influence of the absorption cross section σ_3 on the THG was investigated in detail. The optimum phase-matching ratio and the phase-matching curve were determined. The dependence of the harmonic power on the fundamental power and the absolute power conversion efficiency were measured. All experimental results were found to be in excellent agreement with theory.

We therefore can draw the following conclusions:

(i) The suggestion of Hodgson *et al.*[1] that autoionizing levels give rise to a further resonant enhancement of THG, is only valid for optically thin systems or for optically thick systems if $\Delta k \gg \sigma_3 N$. This has to be considered also for the study of autoionizing states using frequency-mixing experiments as done by Sorokin *et al.*[24]

(ii) In order to get the highest possible conversion efficiency for a given input intensity Φ_1, NL has to be optimized in a phase-matched system. In this case one should aim at an optical depth $\tau \simeq 1$ where the adjacent autoionizing level which is also responsible for strong absorption, is no longer advantageous by increasing the nonlinear susceptibility $\chi_T^{(3)}$ but may even deteriorate the conversion efficiency.

Our experiments have so far been restricted to intensities where no saturation phenomena are detected. Based on this understanding quantitative investigations of saturation phenomena already observed above 10^7 W/cm^2, are in progress.

[1]R. T. Hodgson, P. P. Sorokin, and J. J. Wynne, Phys. Rev. Lett. 32, 343 (1974).
[2]J. R. Taylor, Opt. Commun. 18, 504 (1976).
[3]K. M. Leung, J. F. Ward, and B. J. Orr, Phys. Rev. A 9, 2440 (1974); J. F. Ward and A. V. Smith, Phys. Rev. Lett. 35, 653 (1975); A. T. Georges, P. Lambropoulos, and J. H. Marburger, Opt. Commun. 18, 509 (1976).
[4]A. T. Georges, P. Lambropoulos, and J. H. Marburger, Phys. Rev. A 15, 300 (1977).
[5]C. C. Wang and L. I. Davis, Phys. Rev. Lett. 35, 650 (1975).
[6]S. C. Wallace and G. Zdasiuk, Appl. Phys. Lett. 28, 449 (1976).
[7]A. I. Ferguson and E. G. Arthurs, Phys. Lett. A 58, 298 (1976).
[8]T. R. Royt and Chi H. Lee, Appl. Phys. Lett. 30, 332 (1977).
[9]G. C. Bjorklund, J. E. Bjorkholm, P. F. Liao, and R. H. Storz, Appl. Phys. Lett. 29, 729 (1976).
[10]G. C. Bjorklund, J. E. Bjorkholm, R. R. Freeman, and P. F. Liao, Appl. Phys. Lett. 31, 330 (1977).
[11]J. F. Young, G. C. Bjorklund, A. H. Kung, R. B. Miles, and S. E. Harris, Phys. Rev. Lett. 27, 1551 (1971); A. H. Kung, J. F. Young, G. C. Bjorklund, and S. E. Harris, *ibid.* 29, 985 (1972).
[12]H. Puell, K. Spanner, W. Falkenstein, W. Kaiser, and C. R. Vidal, Phys. Rev. A 14, 2240 (1976).
[13]P. P. Bey, J. F. Giuliani, and H. Rabin, Phys. Rev. Lett. 19, 819 (1967).
[14]N. Van Tran, J. H. McFee, and C. K. N. Patel, Phys. Rev. Lett. 21, 735 (1968).
[15]C. R. Vidal and F. B. Haller, Rev. Sci. Instrum. 42, 1779 (1971).
[16]E. A. Stappaerts, G. W. Bekkers, J. F. Young, and S. E. Harris, IEEE Quantum Electron. 12, 330 (1976).
[17]U. Fano, Phys. Rev. 124, 1866 (1961).
[18]J. A. Armstrong and J. J. Wynne, Phys. Rev. Lett. 33, 1183 (1974); see also Comment by L. Armstrong, Jr. and B. L. Beers, Phys. Rev. Lett. 34, 1290 (1975).
[19]C. E. Moore, *Atomic Energy Levels*, U. S. Natl. Bur. Stand. Cir. No. 467 (U. S. GPO, Washington, D. C., 1952), Vol. 2; P. Esherick, Phys. Rev. A 15, 1920 (1977).
[20]A. Lurio, R. L. Dezafra, and R. J. Goshen, Phys. Rev. 134, A1198 (1964).
[21]M. G. Kozlov and G. P. Startsev, Opt. Spectrosc. 28, 6 (1969).
[22]C. R. Vidal and J. Cooper, J. Appl. Phys. 40, 3370 (1969).
[23]R. D. Hudson, V. L. Carter, and P. A. Young, Phys. Rev. 180, 77 (1969).
[24]P. P. Sorokin, J. J. Wynne, J. A. Armstrong, and R. T. Hodgson, Ann. N. Y. Acad. Sci. 267, 30 (1976).
[25]J. Koch, in *Landolt-Börnstein, Zahlenwerte und Funktionen*, edited by K. H. and A. M. Hellwege (Springer, Berlin, 1962), Vol. 2/8, pp. 6–885.
[26]J. Ducuing and N. Bloembergen, Phys. Rev. 133, 1493 (1964).